IOPscience iopscience.iop.org

Home Search Collections Journals About Contact us My IOPscience

Optically transparent thin-film transistors based on 2D multilayer MoS_2 and indium zinc oxide electrodes

This content has been downloaded from IOPscience. Please scroll down to see the full text.

2015 Nanotechnology 26 035202

(http://iopscience.iop.org/0957-4484/26/3/035202)

View the table of contents for this issue, or go to the journal homepage for more

Download details:

IP Address: 163.180.144.80
This content was downloaded on 30/12/2014 at 19:50

Please note that terms and conditions apply.

Nanotechnology **26** (2015) 035202 (5pp)
doi:10.1088/0957-4484/26/3/035202

Optically transparent thin-film transistors based on 2D multilayer MoS_2 and indium zinc oxide electrodes

Junyeon Kwon[1,4], Young Ki Hong[1,4], Hyuk-Jun Kwon[2], Yu Jin Park[3], Byungwook Yoo[3], Jiwan Kim[3], Costas P Grigoropoulos[2], Min Suk Oh[3] and Sunkook Kim[1]

[1] Multi-Functional Bio/Nano Lab., Kyung Hee University, Gyeonggi 446-701, Korea
[2] Department of Mechanical Engineering, University of California, Berkeley, CA 94720, USA
[3] Display Convergence Research Center, Korea Electronics Technology Institute, Gyeonggi 463-816, Korea

E-mail: ohms@keti.re.kr and seonkuk@khu.ac.kr

Received 20 September 2014, revised 12 November 2014
Accepted for publication 18 November 2014
Published 30 December 2014

Abstract

We report on optically transparent thin film transistors (TFTs) fabricated using multilayered molybdenum disulfide (MoS_2) as the active channel, indium tin oxide (ITO) for the back-gated electrode and indium zinc oxide (IZO) for the source/drain electrodes, respectively, which showed more than 81% transmittance in the visible wavelength. In spite of a relatively large Schottky barrier between MoS_2 and IZO, the *n*-type behavior with a field-effect mobility (μ_{eff}) of $1.4\ cm^2\ V^{-1}\ s^{-1}$ was observed in as-fabricated transparent MoS_2 TFT. In order to enhance the performances of transparent MoS_2 TFTs, a picosecond pulsed laser was selectively irradiated onto the contact region of the IZO electrodes. Following laser annealing, μ_{eff} increased to $4.5\ cm^2\ V^{-1}\ s^{-1}$, and the on-off current ratio (I_{on}/I_{off}) increased to 10^4, which were attributed to the reduction of the contact resistance between MoS_2 and IZO.

Keywords: transition metal dichalcogenides, transparent electronics, MoS_2, TFT, laser annealing

(Some figures may appear in colour only in the online journal)

1. Introduction

The growing desire for a next-generation display has given rise to persistent attempts and efforts to demonstrate optically transparent and mechanically flexible thin-film transistors (TFTs). For a transparent display, a fully transparent thin-film transistor will play an essential role to achieve high transmittance because the TFT backplane in the display has been one of the major factors of reduction in transmittance [1]. In this regard, various new classes of nanomaterials, such as single-walled carbon nanotubes (SWCNTs) or oxide nanowires (NWs), with transparent electrodes have been proposed to achieve ultra-high optical transparency and superior electrical performance due to these one-dimensional semiconductors of molecular thickness [2–8]. Despite the significant progress, a critical weakness remains and must be further improved in their commercial integrated circuit. The challenges to reach a commercial display requires a novel nano-semiconductor to achieve optical transparency, high-mobility and amenability to a large-area growth technique.

Recently, a series of transition metal dichacogenides (TMDCs), especially two-dimensional (2D) molybdenum disulfide (MoS_2), can be an attractive candidate for transparent electronics due to their relatively high mobility (>$80\ cm^2\ V^{-1}\ s^{-1}$), finite bandgap (1–2 eV) and ultra-thin 2D layered structure [9–14]. 2D layered MoS_2 transistors have been well studied as the architecture of the Schottky device in which source/drain metals were directly deposited on active channels of TMDC. To date, the *n*-type behavior of the MoS_2 transistor results in the fact that the Fermi level of the source/drain metal is pinned in the vicinity of the conduction band of MoS_2; thus, a relatively low work-function metal, such as

[4] These authors contributed equally to this work.

 © 2015 IOP Publishing Ltd Printed in the UK

titanium (Ti) or Scandium (Sc), brings about the small Schottky barrier (SB) height to the conduction band [13–17]. However, the conventional transparent metals, indium tin oxide (ITO) or indium zinc oxide (IZO), have the high work function with a work function of ~5.1 eV [18, 19]. The large SB height with the IZO-contacted MoS_2 transistor has limits in its use in the high-performance of transparent devices [20].

Here, we explore transparent multilayer MoS_2 TFTs with ITO for the back-gated electrode and IZO for the source/drain electrodes, respectively. In order to realize the high performance of the transparent MoS_2 transistor, selective laser annealing enables the achievement of superb interfacial characteristics between the IZO electrode and MoS_2 material contact surface and is also useful for a reduction in contact resistance. The irradiation of a pulsed laser with high energy density and a short wavelength onto transparent electrodes leads to the thermal annealing effect at the locally confined small area that needs high temperature without extreme thermal damage. The electrical properties of the laser-annealed transparent MoS_2 TFTs were clearly enhanced, and the average transmittance in the overall devices was estimated at ~81% in the visible wavelength range.

2. Experimental

Figure 1(a) presents a three-dimensional (3D) schematic illustration of the transparent multilayer-MoS_2 TFT with a back-gated structure in a cross-sectional view. The ITO glass with a ITO thickness of 200 nm and a sheet resistance of 10–15 Ω sq^{-1}, respectively, was used as the back-gated electrode of the TFTs. A 300 nm thick SiO_2 as the gate dielectric was deposited on the ITO glass by plasma-enhanced chemical vapor deposition (Low Stress PECVD, SLP-730 by Unaxis) at 350 °C. Mechanically exfoliated multilayer MoS_2 from bulk MoS_2 (SPI supplies, USA) is transferred on the SiO_2 layer [13, 14]. Then, the IZO layer with a thickness of 100 nm as the source/drain electrodes was deposited by sputtering. The IZO source/drain electrodes with various channel lengths were fabricated using conventional photolithography and the etching method. Figure 1(b) shows the transmission spectra (Agilent 8453 UV–vis Spectrophotometer) of transparent MoS_2 TFTs on the glass substrate and on the ITO glass in the 300–900 nm wavelength range. The 1×1 cm^2 area contains 2240 transistor patterns, and about 92% of the area is covered with IZO electrodes. It should be noted that multilayer MoS_2 flakes were randomly distributed in our device configuration. However, the active layer of each TFT in the driving circuitry (for example, six transistors and two capacitors) occupies very limited space in the whole display panel. Also, the overall transmittance of the patterned active layer (e.g. discontinuous layer structure) would be correlated with the summation of each active area. In addition, the reduction of transmittance due to the signal line between the TFT circuit and light-emitting component also plays the important role of estimating the optical transparency of the display panel. So, we believe that our device configuration could evaluate the potential optical transparency of transparent TFT arrays, which have a similar area of the total active layer. The averaged transmittances of our transparent MoS_2 TFTs and ITO glass were ~81% and ~87%, respectively, in the visible wavelength range. The transmittance of MoS_2 TFTs was almost comparable to that of ITO glass in the wavelength range of 450–650 nm, which was most sensitive to response of the human eye. An optical microscope image (Olympus BX51M) of the transparent MoS_2 TFTs on printed texts are presented in figure 1(c). We can clearly identify the texts through the MoS_2 TFTs as well as through the colored IZO electrodes. The inset of figure 1(c) shows a single TFT that consists of a multilayered MoS_2 flake between the IZO source/drain electrodes.

Figure 2(a) represents the schematic illustration of the selective laser annealing process at the contact regions between MoS_2 and the source/drain electrodes using an yttrium vanadate (Nd:YVO_4) picosecond pulsed laser (Newport Corp., USA) operating at a wavelength of 355 nm, a pulse repetition rate of 80 MHz, a pulse width based on the full width at half maximum of 12 ps and a power of 26.8 mW, respectively. The short wavelength (355 nm) helps the transparent electrode efficiently absorb more energy from the incident light of the laser. The 100 nm thickness of IZO showed 30–36% transmittance at 355 nm [21]. 64–70% of the laser energy would be absorbed in the IZO electrodes, and the rest of the energy might reach, and be absorbed in, the MoS_2 layer. In addition, the high repetition rate (80 MHz) causes heat accumulation effects because the temperature cannot cool down to below the working ambient temperature before the next pulse arrives [22]. The accumulated heat is enough to induce changes of the interfacial characteristics of IZO-MoS_2 and might have led to a possible laser annealing process. The Gaussian-type laser beam with a diameter of 1.5 μm was mainly irradiated along the edge of the contact of the target sample placed on a high-resolution *x-y* positioning stage (Aerotech Inc., USA). The laser power, scan speed of the stage, optical shutter and beam path were simultaneously operated by a computer during the annealing process. The details of the experimental conditions were reported earlier [23].

3. Results and discussion

The source-drain current and voltage (I_{ds}–V_{ds}) characteristic curves of the transparent MoS_2 TFT as two-terminal devices (gate was grounded, i.e. at $V_{gs} = 0$ V) before and after laser annealing are compared in figure 2(b). The I_{ds}–V_{ds} characteristic curves of the pristine (before laser annealing) transparent MoS_2 TFT showed typical *n*-type diode-like behavior, and the current level of the device was dramatically increased after laser annealing treatment. In order to investigate the change of the charge transport due to the laser annealing, the I_{ds}–V_{ds} characteristic curves of the transparent MoS_2 TFT ($V_g = 0$ V) were re-plotted using the logarithmic scale, as shown in the inset of figure 2(b). For pristine transparent MoS_2 TFT, two distinct regimes, depending on the slopes of the I_{ds} at $V_g = 0$ V, were observed. In a low-

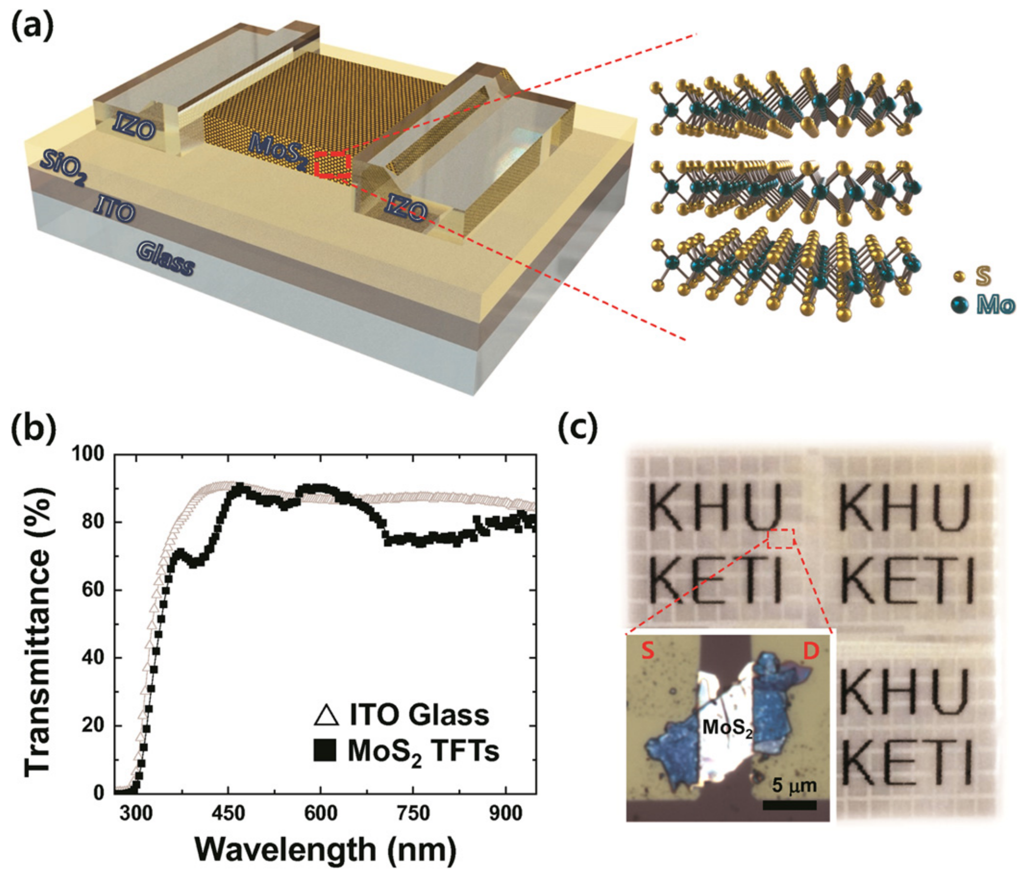

Figure 1. (a) 3D cross-sectional schematic view of the transparent multilayered MoS_2 TFT. The dashed red line indicates atomic arrangements and a layered structure in multilayer MoS_2. (b) Transmission spectra of the ITO glass (△) and the transparent MoS_2 TFTs (■) in the visible wavelength range. (c) Optical microscope image of the transparent MoS_2 TFTs on the printed texts. Inset: magnified optical microscope image of a single TFT consisting of a MoS_2 flake between the IZO source and drain electrodes.

biased region, the I_{ds} increased linearly ($I \propto V$), indicating the ohmic conduction due to the thermionic emission. However, the I_{ds} increased quadratically ($I \propto V^2$) in the high-biased region, which could be explained through the space charge limited current model [24, 25]. Kwon *et al* reported on the decrease of the Schottky barrier width in the picosecond laser-annealed MoS_2 TFT with titanium-gold electrodes, which resulted in the reduction of the contact resistance between MoS_2 and the metal electrodes [23]. The enhancement of the current level and the change of the slopes in the log-log plot of the I_{ds}–V_{ds} characteristic curves suggested that charge carriers would be more effectively injected from the IZO electrode to the MoS_2 active layer due to the laser annealing process, which well agreed with the previous reports [23–25].

Figures 3(a) and (b) show the comparison of the transfer and output characteristic curves of the transparent MoS_2 TFT with respect to the laser annealing process. It is noted that the electrical characteristics were measured in the same MoS_2 TFT for investigating the effects of the laser annealing treatment. As shown in figure 3(a), the field effect mobility ($\mu_{eff} = Lg_m/WC_{ox}V_{ds}$) of the as-fabricated MoS_2 TFT was calculated as $1.4\ cm^2\ V^{-1}\ s^{-1}$ in the linear region ($V_{ds} = 1$ V). It has been known that there exists a large Schottky barrier (~0.7 eV) between IZO and MoS_2 due to the high work function of IZO (~5 eV), which can severely restrict electron transport at source/drain contacts. Recently, Hinkle *et al* reported that the electronic properties of multilayered MoS_2 could be significantly varied with the spatial point even within the same sample [16]. Depending on the stoichiometric variation of sulfur to the molybdenum ratio, the intrinsic defects of the natural MoS_2 could be categorized into S-rich (S: Mo = 2.3:1) and S-deficient (1.8:1) species, which would result in *p*-type and *n*-type characteristics, respectively [16, 26]. The S-deficient defects were estimated to metallic-like properties with a relatively low effective work function, which lead to the inhomogeneous interface between IZO and MoS_2. Although a relative low density of 0.1–5%, lowering of the Schottky barrier height due to the S-deficient defects could be attributed by considering a parallel conduction model [16]. The *n*-type behaviors of the electrical properties, observed in figures 2 and 3, indicated that S-deficient defects would be dominant in the MoS_2 active layer in our transparent TFT. Das *et al* reported that the Fermi levels of metals with high work functions, such as nickel (5.0 eV) and platinum (5.9 eV), were also pinned in the conduction band edge of the MoS_2 [15]. So, the *n*-type behavior of the transparent MoS_2 TFTs could also be attributed to the Fermi level pinning between the MoS_2 and IZO [15].

The laser annealing treatment allowed about fivefold enhancement of the on-current (I_{on}), while the off-current

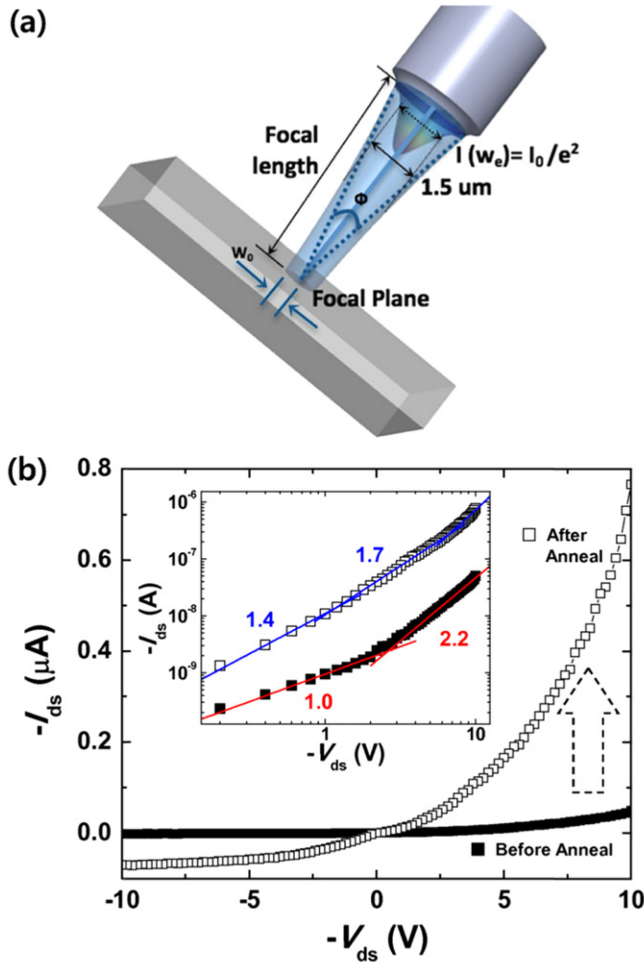

Figure 2. (a) Schematic illustration of the selective laser annealing process. (b) Comparison of the I_{ds}–V_{ds} characteristic curves of transparent MoS_2 TFT at $V_g = 0$ V before (■) and after (□) laser annealing. Inset: I_{ds}–V_{ds} characteristic curves of transparent MoS_2 TFT ($V_g = 0$ V) using the logarithmic scale.

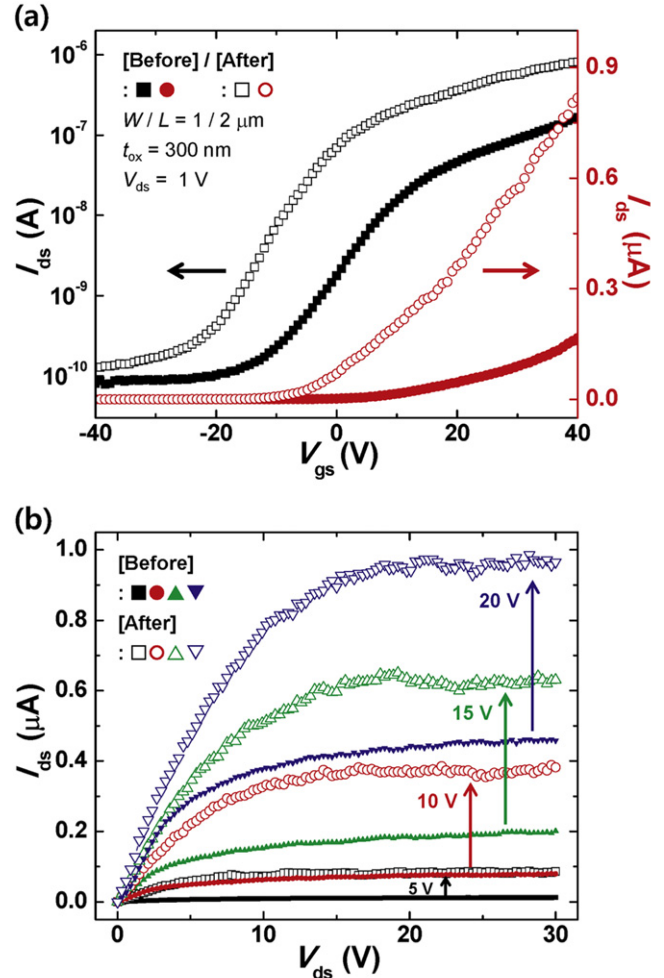

Figure 3. (a) Transfer characteristic curves (V_{gs}–I_{ds}) of the transparent MoS_2 TFT at $V_{ds} = 1$ V before (solid) and after (open symbols) laser annealing. The channel length (L) and width (W) were equal to 2 and 1 μm, respectively. (b) Output characteristic (V_{ds}–I_{ds}) curves of the transparent MoS_2 TFT with different gate biases ($V_{gs} = 5$, 10, 15 and 20 V) before (solid) and after (open symbols) laser annealing.

(I_{off}) levels of the device were hardly changed. The on/off current ratio (I_{on}/I_{off}) of the laser annealed device approached $\sim 10^4$. After the laser annealing treatment, the field effect mobility of the device was threefold increased (4.5 $cm^2 V^{-1} s^{-1}$). Based on the output characteristic curves of the MoS_2 TFT shown in figure 3(b), the improvement of the contact behavior in the low V_{ds} region and the robust current saturation at the high V_{ds} region were observed after laser annealing. The enhancement of the TFT performances due to the laser annealing treatment was in good agreement with the results shown in figure 2. It is known that the composition of the IZO film is changed over 300 °C [27], which can be induced at the IZO-MoS_2 interface by laser annealing. There seems to be oxygen poor environments at the bottom of the IZO electrode at the IZO-MoS_2 interface in which an oxygen deficient defect can be produced by heat generated through laser annealing. The conductivity of the interfacial side in IZO electrodes would increase due to these oxygen deficient defects, resulting in the reduction of contact resistance between IZO and MoS_2 [28, 29].

4. Conclusion

In conclusion, we successfully fabricated transparent multi-layered MoS_2 TFTs using conventional transparent conducting oxide electrodes such as ITO and IZO. Our transparent TFTs showed more than 81% transmittance in the visible wavelength range. Even taking into account the high work function of IZO, the transparent MoS_2 TFTs exhibited quite moderate electrical performances because of the intrinsic defects in natural MoS_2, which would play a role in lowering the Schottky barrier height. In order to boost the electrical performances of those samples, the picosecond laser annealing treatment was selectively applied onto the contact regions between the MoS_2 and IZO source/drain electrodes. As a result, the field-effect mobility and the on/off current ratio of the transparent MoS_2 TFTs approached up to 4.5 $cm^2 V^{-1} s^{-1}$ and $\sim 10^4$, respectively. Although future works will include controlling the defects' concentration and optimizing the electrical properties as well as the transmittance, these results

indicate potential possibilities for applications in future transparent display devices using multilayer MoS_2 TFTs with conventional IZO contacts.

Acknowledgement

This research was supported by the Industrial Strategic Technology Development Program (10045145) and the Basic Science Research Program (2012R1A1A1042630).

References

[1] Facchetti A and Marks T J 2010 *Transparent Electronics: From Synthesis to Applications* (Chichester: Wiley)

[2] Kim S, Ju S, Back J H, Xuan Y, Ye P D, Shim M, Janes D B and Mohammad S 2009 Fully transparent thin-film transistors based on aligned carbon nanotube arrays and indium tin oxide electrodes *Adv. Mater.* **21** 564–8

[3] Kim S, Kim S, Park J, Ju S and Mohammadi S 2010 Fully transparent pixel circuits driven by random network carbon nanotube transistor circuitry *ACS Nano* **4** 2994–8

[4] Sajed F and Rutherglen C 2013 All-printed and transparent single walled carbon nanotube thin film transistor devices *Appl. Phys. Lett.* **103** 143303

[5] Ju S *et al* 2008 Transparent active matrix organic light-emitting diode displays driven by nanowire transistor circuitry *Nano Lett.* **8** 997–1004

[6] Nasr B, Wang D, Kruk R, Rösner H, Hahn H and Dasgupta S 2013 High-speed, low-voltage, and environmentally stable operation of electrochemically gated zinc oxide nanowire field-effect transistors *Adv. Funct. Mater.* **23** 1750–8

[7] Hecht D S, Hu L and Irvin G 2011 Emerging transparent electrodes based on thin films of carbon nanotubes, graphene, and metallic nanostructures *Adv. Mater.* **23** 1482–513

[8] Chen D, Liu Z, Liang B, Wang X and Shen G 2012 Transparent metal oxide nanowire transistors *Nanoscale* **4** 3001–12

[9] Radisavljevic B, Radenovic A, Brivio J, Giacometti V and Kis A 2011 Single-layer MoS_2 transistors *Nat. Nanotechnol.* **6** 147–50

[10] Mak K F, Lee C, Hone J, Shan J and Heinz T F 2010 Atomically thin MoS_2: a new direct-gap semiconductor *Phys. Rev. Lett.* **105** 136805

[11] Wang Q H, Kalantar-Zadeh K, Kis A, Coleman J N and Strano M S 2012 Electronics and optoelectronics of two-dimensional transition metal dichalcogenides *Nat. Nanotechnol.* **7** 699–712

[12] Chhowalla M, Shin H S, Eda G, Li L J, Loh K P and Zhang H 2013 The chemistry of two-dimensional layered transition metal dichalcogenide nanosheets *Nat. Chem.* **5** 263–75

[13] Choi W *et al* 2012 High-detectivity multilayer MoS_2 phototransistors with spectral response from ultraviolet to infrared *Adv. Mater.* **24** 5832–6

[14] Kim S *et al* 2012 High-mobility and low-power thin-film transistors based on multilayer MoS_2 crystals *Nat. Commun.* **3** 1011

[15] Das S, Chen H Y, Penumatcha A V and Appenzeller J 2013 High performance multilayer MoS_2 transistors with scandium contacts *Nano Lett.* **13** 100–5

[16] McDonnell S, Addou R, Buie C, Wallace R M and Hinkle C L 2014 Defect-dominated doping and contact resistance in MoS_2 *ACS Nano* **8** 2880–8

[17] Lopez-Sanchez O, Lembke D, Kayci M, Radenovic A and Kis A 2013 Ultrasensitive photodetectors based on monolayer MoS_2 *Nat. Nanotechnol.* **8** 497–501

[18] Cui J, Wang A, Edleman N L, Ni J, Lee P, Armstrong N R and Marks T J 2001 Indium tin oxide alternatives—high work function transparent conducting oxides as anodes for organic light-emitting diodes *Adv. Mater.* **13** 1476–80

[19] Minami T 2005 Transparent conducting oxide semiconductors for transparent electrodes *Semicond. Sci. Technol.* **20** S35–44

[20] Chuang S *et al* 2014 MoS_2 P-type transistors and diodes enabled by high work function MoO_x contacts *Nano Lett.* **14** 1337–42

[21] Kim H M, Jung S K, Ahn J S, Kang Y J and Je K C 2003 Electrical and optical properties of In_2O_3-ZnO films deposited on polyethylene terephthalate substrates by radio frequency magnetron sputtering *Jpn. J. Appl. Phys.* **42** 223–7

[22] Eaton S M, Zhang H, Herman P R, Yoshino F, Shah L, Bovatsek J and Arai A Y 2005 Heat accumulation effects in femtosecond laser-written waveguides with variable repetition rate *Opt. Express* **13** 4708–16

[23] Kwon H J, Choi W, Lee D, Lee Y, Kwon J, Yoo B, Grigoropoulos C P and Kim S 2014 Selective and localized laser-anneal effect for high-performance flexible multilayer MoS_2 thin-film transistors *Nano Res.* **7** 1137–45

[24] Kao K C and Hwano W 1981 *Electrical Transport in Solids* (New York: Pergamon)

[25] Lampert M A 1956 Simplified theory of space-charge-limited currents in an insulator with traps *Phys. Rev.* **103** 1648–56

[26] Zhou W, Zou X, Najmaei S, Liu Z, Shi Y, Kong J, Lou J, Ajayan P M, Yakobson B I and Idrobo J C 2013 Intrinsic structural defects in monolayer molybdenum disulfide *Nano Lett.* **13** 2615–22

[27] Taylor M P *et al* 2008 The remarkable thermal stability of amorphous In-Zn-O transparent conductors *Adv. Funct. Mater.* **18** 3169–78

[28] Fujii M, Ishikawa Y, Ishihara R, Van Der Cingel J, Mofrad M R T, Horita M and Uraoka Y 2013 Low temperature high-mobility InZnO thin-film transistors fabricated by excimer laser annealing *Appl. Phys. Lett.* **102** 122107

[29] Ahn S E, Ji H J, Kim K, Kim G T, Bae C H, Park S M, Kim Y K and Ha J S 2007 Origin of the slow photoresponse in an individual sol-gel synthesized ZnO nanowire *Appl. Phys. Lett.* **90** 153106